*J. Fluid Mech.* (1992), *vol.* 239, *pp.* 429–448
*Printed in Great Britain*



# Melting and dissolving

By ANDREW W. WOODS

Institute of Theoretical Geophysics, Department of Applied Mathematics and Theoretical Physics, University of Cambridge, Silver Street, Cambridge CB3 9EW, UK

(Received 28 December 1990 and in revised form 8 October 1991)

The diffusion-governed melting that occurs when a binary melt is placed in contact with a pure solid is described. It is shown that if the melt superheat is much greater than the solid supercooling, the melt composition at the interface equals that of the solid and so the solid will *melt* at a rate determined by the thermal diffusivity. However, as the liquid superheat decreases, chemical disequilibrium may lower the interface temperature and so the melt composition at the interface increases above that of the solid, according to the liquidus relation. In this case the solid will *dissolve* into the liquid at a rate determined by the solutal diffusivity. These diffusion-governed solutions are used to infer the different modes of convection which may rise when the interface between the solid and the melt is horizontal.

The theory is generalized to investigate the diffusion-governed melting of a binary solid solution placed in contact with a binary melt. If the melt superheat is sufficient then the rate of phase change is again determined by the thermal diffusivity. In this case, owing to the very small solutal diffusivity in both the solid and the liquid, the melt composition at the interface is nearly equal to that of the solid. This corresponds to the melting regime. As the liquid superheat decreases, the rate of phase change decreases to values determined by the solutal diffusivity in the liquid, and the melt composition at the interface evolves towards that of the far-field liquid. This corresponds to the dissolving regime. As the melt superheat decreases further, with the solid still changing phase into liquid, then the melt composition at the interface remains approximately equal to that of the far-field melt. In each case, a compositional boundary layer develops in the solid, just ahead of the interface, in order to restore the solid at the interface to thermodynamic equilibrium. These different phase change regimes may arise if the composition of the solid is either higher or lower than that of the liquid.

## 1. Introduction

Cold ice cubes can *melt* in warm salty water, with the latent heat of melting supplied by the warm water; however, relatively warm ice cubes can *dissolve* in cold, salty water with the latent heat of melting supplied by the ice. This is possible because ice has a range of equilibrium temperatures in aqueous salt solutions. Melting occurs when the heat flux supplied from the hot liquid to the interface exceeds the heat flux which can be conducted away from the interface into the cold solid. In contrast, dissolving occurs in order to restore the melt near the interface with the solid to (chemical) thermodynamic equilibrium. For example, there is no phase change when pure ice at 0 °C is placed in contact with pure water at 0 °C; however, pure ice at −1 °C may dissolve if placed in contact with salty water at −1 °C. In many systems, the solutal diffusivity is much smaller than the thermal

diffusivity and so melting is rate limited by heat transfer while dissolving is rate limited by solute transfer.

In this paper, we systematically investigate the effects of a variable melting temperature upon the melting process, motivated by their importance in many situations. For example, in active volcanic regions, hot molten magmas may come into contact with the cold wall rock of magma chambers several kilometres below the surface of the Earth's crust. The mixing, melting and solidifying which ensues is central to the geochemical interpretation of solidified igneous intrusions and also the deposits from volcanic eruptions (Huppert & Sparks 1988*b*). Ice formations in the ocean may undergo significant volume changes due to the ice-pump effect, in which the variation of melting point with depth (pressure) allows upwelling/downwelling water to melt or freeze (Lewis & Perkins 1986); an understanding of the oceanic ice budget provides important constraints upon global climate modelling.

There have been many investigations of Stefan phase change problems; however, these have mainly focused upon mono-component systems (e.g. Hill 1987). Recently, the effects of (i) compositional differences between the solid and the melt and (ii) fluid convection in the melt have been studied, particularly in the context of solidification (Huppert & Worster 1985; Woods & Huppert 1989, Kerr *et al.* 1989). There have also been a number of studies of the role of fluid convection upon melting. Huppert (1989) investigated the phase changes which occur during the forced turbulent flow of a hot fluid over a cold solid surface. When the solid and liquid have different, fixed melting and freezing temperatures, there are several different regimes in which the fluid solidifies or the solid melts as a consequence of the turbulent heat transfer from the fluid to the solid. When the heat transfer from the melt is through fluid convection, Huppert (1989) showed that in many situations solidification occurs first followed by melting; this phenomenon has been confirmed in a recent study of Bruce & Huppert (1989). Huppert & Sparks (1988*a*, *b*) investigated experimentally and theoretically the melting of solid into an underlying hot melt in the cases in which (i) there is separate thermally driven melt convection in the layer of melt and also the underlying liquid, as in a double-diffusive system (cf. Turner 1979) and (ii) there is one well-mixed layer of thermally convecting melt below the solid. They reported melting rates which were significantly larger than those in a purely diffusive regime due to the more efficient convective heat supply from the melt. In a third paper, Huppert & Sparks (1988*c*) extended the experimental results of Campbell (1986) and Fang & Hellawell (1988) in which the floor of a chamber was melted by an overlying layer of hot but less dense melt. Woods (1991) reconsidered this situation and developed a simple quantitative model of the melting, driven by compositional convection, which agrees well with the experiments.

In the present paper we focus upon the effects of compositional differences between the solid and the melt. We analyse theoretically the *diffusion*-governed melting of a pure solid into a binary melt. Initially, we consider the case in which the solidus is independent of composition, so that the maximum melting temperature of the solid does not vary with the composition of the solid, as is the case in aqueous salt solutions. We note that the solid may change phase at lower temperatures if it is in contact with a binary liquid, and that the temperature of the interface is determined by the liquidus relationship. We distinguish between two forms of phase change. In the first, which we call melting, the rate of phase change is determined by the thermal diffusivity; in the second, the rate of phase change is determined by the compositional diffusivity and we call this dissolving. We show that in the dissolving regime, relatively warm solid may dissolve into a relatively cold liquid. We calculate the

difference between the density of the melt at the solid interface and the density of the liquid far from the interface in order to determine the nature of the convection which may arise as the geometry and melt composition are varied.

In §4, we generalize the analysis by considering binary solid solutions. In this case, the melting temperature of the solid phase depends upon its composition; we discuss the conditions under which melting and dissolving may arise. In §5, we summarize the main results of our study.

## 2. Diffusion-governed melting

We analyse the diffusion-governed melting of a pure solid of end-member composition $A$ and initial uniform temperature $T_s$ by an adjacent layer of binary melt of composition $C_m$ and temperature $T_m$ (figure 1). The composition is defined to be the mass fraction of the end-member $B$ in the material. Therefore $C_s = 0$. We assume that the process satisfies the constraints of thermodynamic equilibrium and that the melt remains static. For simplicity we consider the solid and melt to fill semi-finite domains; the solutions obtained from this approach will be valid in a finite domain up to the time when the thermal effects reach the edge of the domain (assuming the thermal diffusivity exceeds that of the composition); beyond such time caution should be exercised in applying the present quantitative results to a finite domain. The equations for the conservation of heat and composition are

$$\frac{\partial T}{\partial t} = \kappa_l \frac{\partial^2 T}{\partial z^2} \quad \text{for} \quad z < h(t), \tag{2.1a}$$

$$\frac{\partial T}{\partial t} = \kappa_s \frac{\partial^2 T}{\partial z^2} \quad \text{for} \quad z > h(t) \tag{2.1b}$$

and

$$\frac{\partial C}{\partial t} = D_l \frac{\partial^2 C}{\partial z^2} \quad \text{for} \quad z < h(t); \qquad C = C_s = 0 \quad \text{for} \quad z > h(t), \tag{2.1c, d}$$

where $\kappa_l$, $\kappa_s$ are the thermal diffusivities of the liquid and solid phases, $D_l$ is the compositional diffusivity in the liquid phase. The position of the interface between the solid and the liquid is $z = h(t)$, with the solid occupying the region $z > h(t)$. For simplicity, we assume that there is no volume change associated with the phase change and that there is no diffusion of composition in the solid. At the interface, $z = h(t)$, the boundary conditions are (Carslaw & Jaegar 1986; Kurz & Fisher 1986)

$$c_l \rho_l \kappa_l \left.\frac{\partial T}{\partial z}\right|_{h-} - c_s \rho_s \kappa_s \left.\frac{\partial T}{\partial z}\right|_{h+} = -L \rho_s \dot{h}, \tag{2.2a}$$

$$D_l \left.\frac{\partial C}{\partial z}\right|_{h-} = -\dot{h}(C_I - C_s) = \dot{h} C_I, \tag{2.2b}$$

and the equilibrium constraint

$$T_I = T_e - \Gamma(C_I - C_e), \tag{2.2c}$$

where $L$ is the latent heat and $\rho_s$, $\rho_l$ the solid and liquid densities. The subscript I represents a value evaluated at the interface and e represents a known reference

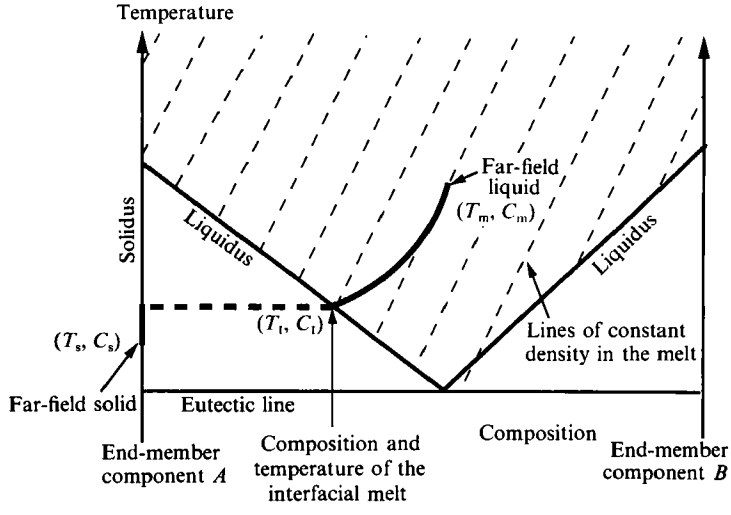


FIGURE 1. Path on the $(T, C)$ phase diagram moving from the far-field solid to the far-field melt; solid portions of the path represent the physical path through the system, while the dotted portion represents the change in composition as we move from solid to melt. In the dimensionless variables of §2, $\hat{C}_m = 1$, $\hat{C}_s = 0$.

point in order to define the liquidus. In (2.2$c$) we have assumed a linear relationship for the liquidus. The situation is sketched in figure 1. The theory may be extended to the general case in which $T_I - T_e$ is a function of $(C_I - C_e)$; however, in most situations, the liquidus may be approximated locally by a linear relationship of the form (2.2$c$).

It is instructive to redefine the temperatures in dimensionless form (denoted by a carat); we set $\hat{T}_L(C_m) = 0$, and scale temperatures relative to $\Gamma C_m$ (i.e. $\hat{T} = (T - \hat{T}_L(C_m))/\Gamma C_m$) and compositions relative to $C_m$ (i.e. $\hat{C} = C/C_m$). Therefore the maximum melting temperature of the solid is unity in dimensionless variables and the superheat of the melt $\hat{T}_m = (T_m - T_L(C_m))/\Gamma C_m$. The system of equations admits a similarity solution in which $h(t) = 2\lambda(\kappa_1 t)^{\frac{1}{2}}$ with similarity variable $\eta = z/(2(\kappa_1 t)^{\frac{1}{2}})$. Here, $\lambda$ is the dimensionless rate of phase change from solid to liquid. The dimensionless temperatures and compositions are given by

$$\hat{T} = \hat{T}_m + \left(\frac{\hat{T}_I - \hat{T}_m}{\operatorname{erfc}(-\lambda)}\right)\operatorname{erfc}(-\eta) \quad \text{for} \quad \eta < \lambda, \tag{2.3$a$}$$

$$\hat{T} = \hat{T}_s + \left(\frac{\hat{T}_I - \hat{T}_s}{\operatorname{erfc}(\lambda/K)}\right)\operatorname{erfc}\left(\frac{\eta}{K}\right) \quad \text{for} \quad \eta > \lambda \tag{2.3$b$}$$

and

$$\hat{C} = 1 + \left(\frac{\hat{C}_I - 1}{\operatorname{erfc}(-\lambda/\epsilon)}\right)\operatorname{erfc}\left(-\frac{\eta}{\epsilon}\right) \quad \text{for} \quad \eta < \lambda, \tag{2.3$c$}$$

and $\hat{C}_I$, $\hat{T}_I$ are determined from the boundary conditions (2.2$a$, $b$) which in non-dimensional form become

$$\hat{C}_I = \epsilon(\epsilon + \lambda F(-\lambda/\epsilon))^{-1}, \tag{2.4$a$}$$

and

$$\left(\frac{1}{F(-\lambda)} + \frac{K\mu}{F(\lambda/K)}\right)\hat{T}_I = \frac{\hat{T}_m}{F(-\lambda)} + \hat{T}_s\frac{K\mu}{F(\lambda/K)} - S\lambda. \tag{2.4$b$}$$

Combining these with (2.2*c*), which may be expressed as $\hat{T}_I + \hat{C}_I = 1$, we obtain the eigenvalue relationship

$$\hat{T}_m = F(-\lambda)\left(S\lambda - \hat{T}_s \frac{\mu K}{F(\lambda/K)} + \left(\frac{1}{F(-\lambda)} + \frac{\mu K}{F(\lambda/K)}\right)\left(\frac{\lambda F(-\lambda/\epsilon)}{\epsilon + \lambda F(-\lambda/\epsilon)}\right)\right), \quad (2.4c)$$

where $F(x) = \pi^{\frac{1}{2}} \exp(z^2) \operatorname{erfc}(x)$, $K = (\kappa_s/\kappa_l)^{\frac{1}{2}}$, $\mu = \rho_s c_s/\rho_m c_m$, $\epsilon = (D_l/\kappa_l)^{\frac{1}{2}} \ll 1$ and the Stefan number $S = \rho_s L/\rho_m c_m \Gamma C_m$. Note that $F(x)$ is tabulated in Carslaw & Jaegar (1986, p. 485). In (2.4*c*), $\hat{T}_m$ and $\hat{T}_s$ are the imposed melt and solid temperatures, and these implicitly determine the rate of phase change $\lambda$ of the solid.

This solution extends that of Huppert & Worster (1985) in that we are considering an infinite, not semi-infinite domain; the significant differences between the following discussion and those of Huppert & Worster (1985) and Worster (1986) arise because we are considering the case in which the solid changes phase into melt, $\lambda > 0$, rather than that of solidification in which $\lambda < 0$. We assume that the solidus is independent of composition and so there is no scope for morphological instability of melting due to superheating of the solid; this is quite different from the solidification problem in which the liquid may become supercooled leading to the formation of a mushy zone.

We now present some simple asymptotic relationships concerning limiting forms of the rate of phase change, $\lambda$, and support the discussion with some numerical solutions. In figure 2 we present numerical calculations of the rate of phase change $\lambda$ as a function of the superheat of the melt, for several values of the Stefan number, $S$. We consider cases in which the solid temperature is (i) greater than ($\hat{T}_s = 0.75$) (ii) equal to ($\hat{T}_s = 0$) and (iii) less than ($\hat{T}_s = -5.0$) the liquidus temperature of the melt.

These figures reveal a number of different aspects of the phase change process. First, we identify conditions under which there is no phase change. In this case, the heat flux supplied to the interface from the melt equals that conducted away from the interface into the solid. We then discuss the effect of increasing the temperature of the melt, and this leads to a natural distinction between melting and dissolving.

### 2.1. *Conditions for no melting*

First, we note from (2.4*a*) that $0 < C_I < 1$ and therefore $0 < T_I < 1$. It follows from (2.4*b*) that when $\hat{T}_s > 0$ the minimum value of the non-dimensional rate of phase change, $\lambda$, satisfies $\lambda_{\min} > 0$. This means that whenever the solid temperature exceeds the liquidus temperature of the far-field liquid, chemical disequilibrium requires that the solid changes phase into melt, as may be seen in figure 2(*a*) in which $\hat{T}_s = 0.75$.

In the case $\hat{T}_s = 0$, figure 2(*b*), there is an equilibrium solution $\lambda = 0$ in which $\hat{T}_s = \hat{T}_m$ and $\hat{C}_I = 1$. As $\hat{T}_m$ is increased, the interfacial temperature increases and hence the interfacial composition decreases. Therefore the solid changes phase in order to accommodate the flux of solute from the far-field liquid and maintain thermodynamic equilibrium.

In the situation in which $\hat{T}_s < 0$ (figure 2*c*) there is an equilibrium state in which there is no melting and the diffusion of heat from the melt into the interface balances the diffusion of heat from the interface into the solid. Again, this requires $\lambda = 0$ and so $\hat{C}_I = 1$ and $\hat{T}_I = 0$. The conservation of heat across the interface may be expressed mathematically from (2.4*b*) as

$$\hat{T}_m = K\mu\hat{T}_s \quad (2.5)$$

We deduce that in order for the solid to change phase when $\hat{T}_s < 0$, the melt must possess superheat, $\hat{T}_m > -K\mu\hat{T}_s$.

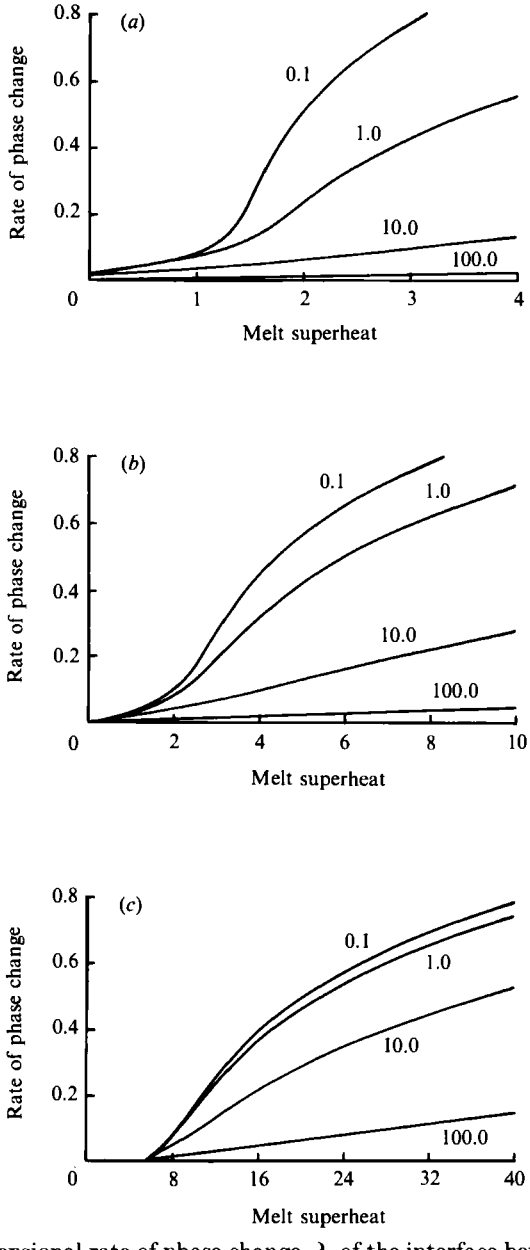


FIGURE 2. Non-dimensional rate of phase change, $\lambda$, of the interface between the solid and the melt as a function of the melt superheat for (*a*) $T_s = 0.75$, (*b*) $T_s = 0$ and (*c*) $T_s = -5.0$. Curves are labelled with four different values of the Stefan number, 0.1, 1.0, 10.0, 100.0, and $\epsilon$ is equal to 0.1.

### 2.2. *The dissolving and melting regimes*

We now consider how the similarity solutions change as the initial temperature of the liquid is increased beyond the equilibrium value given by (2.5), and the solid changes phase into melt. At the equilibrium temperature, the interface composition equals that of the far-field liquid; therefore, as the liquid temperature is increased and hence the interface temperature increases, the interface composition must decrease in order to remain in thermodynamic equilibrium. While the interface composition exceeds

that of the solid, solute must diffuse from the far-field liquid to the interface in order to effect this change in composition. Therefore the rate of phase change is limited by the rate at which composition may diffuse from the far field to the interface. We describe this process as *dissolving*. As the liquid temperature is increased from the equilibrium value, the interface temperature also increases, and so the heat flux which may be conducted away into the solid increases. This tends to suppress any increase in the rate of phase change and so initially the rate of phase change only increases relatively slowly.

However, for sufficiently large liquid superheat, the interface composition becomes approximately equal to that of the solid, the interface temperature becomes fixed and the rate of phase change is no longer constrained by the need to diffuse solute from the liquid to the interface. Therefore, since the interface conditions are fixed, on increasing the liquid temperature further, the rate of phase change increases more rapidly per unit increase in liquid temperature. We describe this phase change regime as *melting* rather than dissolving. In figure 2, the points of inflexion correspond to the smallest far-field liquid temperature at which the composition of the interface melt is approximately equal that of the solid; for liquid temperatures greater than this value, the phase change process becomes one of melting rather than dissolving.

*The dissolving regime*

In the limit $0 < \hat{T}_m + K\mu\hat{T}_s \ll 1$, which corresponds to a small perturbation from the equilibrium state, (2.5), we expect that the rate of phase change is small. Guided by the above qualitative description of dissolving, we now show that the rate of phase change is indeed limited by the diffusion of solute in the liquid. In this limit, (2.4*b*) implies that the interface temperature $\hat{T}_I \sim \hat{T}_m + K\mu\hat{T}_s/(1+K\mu) < 1$, assuming $S = O(1)$ as is usually the case. However, the liquidus relation $\hat{C}_I + \hat{T}_I = 1$ now requires that $1 - \hat{C}_I < 1$. Therefore, from (2.4*a*), we deduce that $\lambda = O(\epsilon)$ and so the rate of melting is determined by the rate of diffusion of composition. Indeed, at time $t$, the molten solid has a thickness $h(t) = 2\lambda(\kappa_1 t)^{\frac{1}{2}} \sim O((Dt)^{\frac{1}{2}})$ and this corresponds to the thickness of the diffusive compositional boundary layer. In contrast, the thermal boundary layer, which scales as $(\kappa_1 t)^{\frac{1}{2}}$, extends far beyond the layer of molten solid and into the original liquid.

We have plotted the thermal and compositional boundary-layer structures appropriate for this dissolving regime in figure 3(*a*). In summary, dissolving occurs in order to maintain the interfacial melt in (chemical) thermodynamic equilibrium, since the composition of the melt at the interface differs from the composition of both the solid and liquid. Furthermore, the rate of production of molten solid is constrained by the rate at which the solute may diffuse from the far field into the newly formed melt.

*The melting regime*

When the temperature of the far-field liquid is greater than that at the inflexion points in figure 2, and

$$\frac{\hat{T}_m}{F(-\lambda)} + \frac{\hat{T}_s K\mu}{F(\lambda/K)} > \frac{1}{F(-\lambda)} + \frac{1}{F(\lambda/K)}, \tag{2.6}$$

then in order that the interface be in thermodynamic equilibrium, with $\hat{T}_I \sim 1$, the equation for the conservation of heat at the interface, (2.4*b*), requires $\lambda \sim O(1)$. We can immediately conclude from (2.3*c*) that, after a time $t$, the thickness of the melt produced from the solid, $h(t) \sim O((\kappa_1 t)^{\frac{1}{2}}) \gg (D_1 t)^{\frac{1}{2}}$. Thus, the solution (2.3*c*) shows that

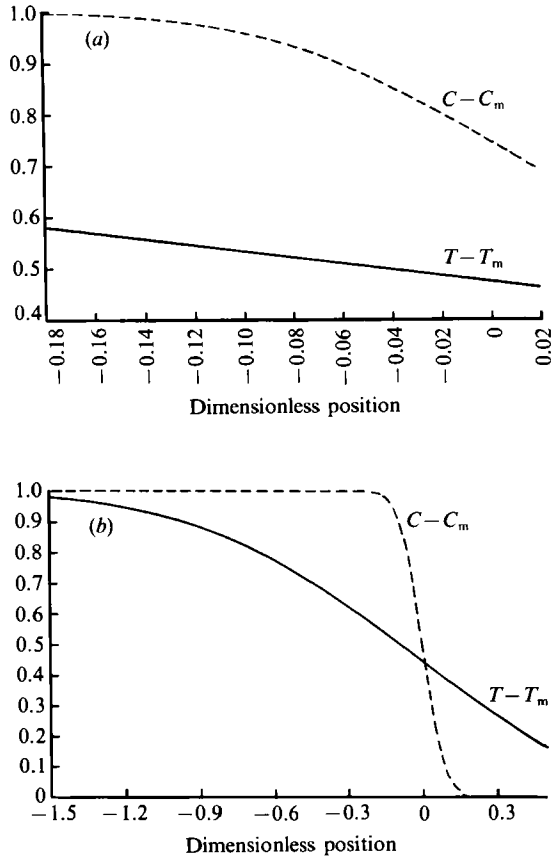


FIGURE 3. Profiles of $T-T_m$ and $C-C_m$ in the melt ahead of the melting interface for (*a*) a dissolving interface ($\lambda = 0.02$) and (*b*) a melting interface ($\lambda = 0.5$). In both cases, $S = 1$ and $\epsilon = 0.1$. In the melt, the dimensionless position, $\eta < \lambda$ ; $\eta = 0$ corresponds to the initial position of the solid/liquid interface. For convenience of plotting, the temperature $T-T_m$ has been re-scaled with respect to the dimensionless far-field melt temperature, which may be deduced from figure 2.

the composition in the melt only varies across a diffusive boundary layer, of thickness $(D_l t)^{\frac{1}{2}}$, which is located at the original position of the interface between the solid and the liquid, $z = 0$. In the layer of molten solid between the actual solid interface and this compositional boundary layer, the composition is virtually identical to that of the solid; in the limit $\lambda \gg \epsilon$ it satisfies

$$\hat{C} \sim \frac{\epsilon}{2\pi^{\frac{1}{2}}\lambda} \sim 0. \tag{2.7}$$

We have plotted a numerical solution showing the structure of the compositional and thermal boundary layers in the melting regime, $\lambda \sim O(1)$, in figure 3(*b*). We can see that the thermal boundary layer extends from the interface between the molten solid and the solid throughout the zone of molten solid, while the compositional boundary layer is localized at the boundary between the molten solid and the original liquid, away from the solid boundary.

In summary, in the melting regime, the composition of the interface equals that of the solid and so the interface temperature is also fixed and equals the liquidus

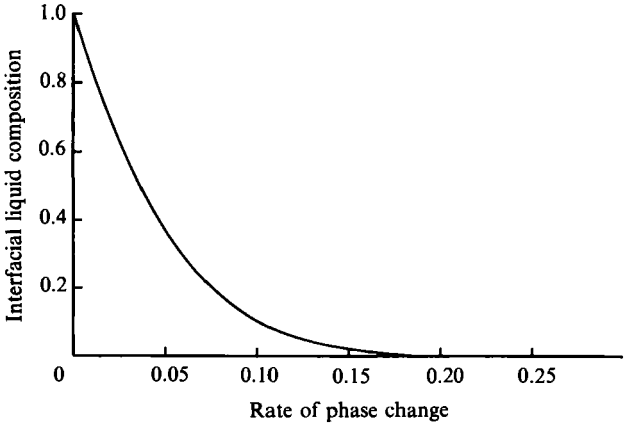


FIGURE 4. Interfacial composition as a function of the rate of phase change $\lambda$. In this figure $\epsilon = 0.1$.

temperature of the solid; therefore, the phase change is driven purely by the superheat of the liquid. Since the melt at the interface has the same composition as the solid, the compositional field does not constrain the rate of growth. In figure 2 it may be seen that for a given superheat, $\lambda$ decreases with $S$ because more thermal energy is required to overcome the latent heat of fusion as the Stefan number increases.

The variation in the composition of the melt at the interface with the rate of phase change is shown in figure 4. For $\lambda \geqslant 0.2$, the melt at the interface has virtually the same composition as the solid, $C_1 \sim 0$, and so this corresponds to the melting regime. Only for smaller values of $\lambda$, does the composition of the melt at the interface differ from that of the solid. In this case the compositional boundary layer extends right up to the solid and the phase change is therefore controlled by compositional diffusion. As may be seen from the location of the points of inflexion in figure 2, the minimum superheat of the liquid required for melting, rather than dissolving, increases with the Stefan number of the liquid.

### 2.3. *Further comments on dissolving*

One interesting feature of these similarity solutions, which arises as a result of the assumption of thermodynamic equilibrium, is that a relatively warm solid may be dissolved by a relatively cold liquid. Such a situation is apparent in figure 2(*a*) in which the initial temperature of the solid $\hat{T}_s = 0.75$; it may be seen that solutions with $\lambda > 0$ exist even when the temperature of the melt satisfies $0 < \hat{T}_m < 0.75$ in which case $\hat{T}_s > \hat{T}_m$. The solid dissolves into the melt to restore the system to equilibrium. The heat required for the phase change is supplied from the solid, whose temperature is greater than the liquidus temperature of the melt. By adding molten solid of pure end-member $A$, which is of lower composition, the melt evolves towards the liquidus and hence equilibrium. If we specify $\hat{T}_s > \hat{T}_m$ then in order that $\lambda > 0$ it follows from (2.4*b*) that $\hat{T}_I < \hat{T}_s$. In this case, (2.4*a*) implies that $\lambda \sim O(\epsilon)$ corresponding to the dissolving regime. Now, however, heat flows from the main body of solid into the interface.

In figure 5, we show how the temperature of the far-field liquid, the interface and the far-field solid are related during dissolving. Dissolving occurs when the composition of the melt at the interface lies between that of the melt and the solid. In figure 5(*a*), the curve labelled (i) represents the line along which the interface and

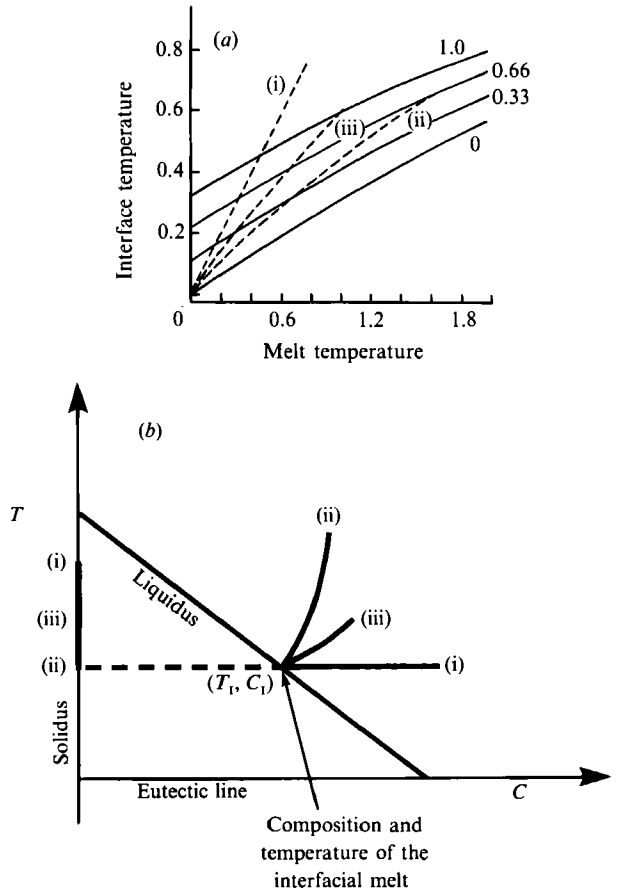


FIGURE 5. (*a*) Temperature of the interface as a function of the temperature of the melt with the initial temperature of the solid, $T_s = 0, 0.33, 0.66, 1.0$ as labelled. The curves labelled (i), (ii) and (iii) respectively correspond to $T_I = T_m$, $T_I = T_s$ and $T_m = T_s$. (*b*) Path in the $(T, C)$ phase diagram corresponding to the curves (i), (ii) and (iii) in (*a*).

the melt have the same temperature. In this case, the solid has a higher temperature, and provides a source of thermal energy to allow a phase change from solid to liquid at the interface. Although there is no heat transfer in the isothermal melt region, there is a solute transfer between the dissolving interface and the melt; this decreases the composition of the liquid near the interface and hence the melt evolves towards the liquidus following the path (i) shown in figure 5(*b*). The line (ii) in figure 5(*a*), represents the line along which the solid and the interface have the same temperature. In this case the melt has a higher temperature than the interface and provides the thermal energy to dissolve the interface. Therefore, in this case, there is diffusion of both heat and solute in the liquid while the solid remains isothermal. The melt now evolves towards the liquidus along the path (ii) shown in figure 5(*b*). The line (iii) on figure 5(*a*), which lies between lines (i) and (ii), represents the line along which the solid and melt have the same temperature. In this case the interface temperature is lower than both the solid and the melt; the thermal energy required to melt the interface is supplied from both the solid and the melt, and the melt evolves towards the liquidus along the intermediate path (iii) shown on figure 5(*b*).

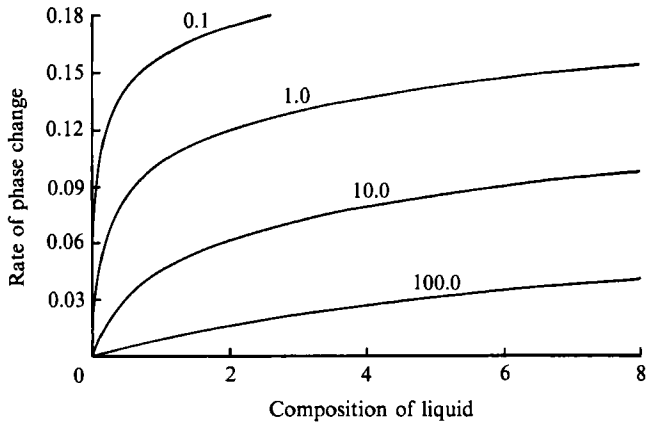


FIGURE 6. The rate of phase change (dissolving) as a function of the composition of the liquid, when both the liquid and solid temperatures equal the maximum melting temperature of the solid. Curves are shown for four Stefan numbers; these are defined by reference to the situation in which the liquid has unit composition.

To clarify the distinction between melting and dissolving, it is instructive to note how the rate of phase change depends upon the compositional difference between the solid and the liquid. In figure 6 we show how the rate of phase change increases as the liquid composition is increased from that of the solid, with all other properties fixed. In the figure we have fixed the far-field temperature of both the liquid and solid to equal the liquidus temperature corresponding to the solid composition, i.e. the maximum temperature at which material can exist as solid. Therefore when the liquid composition is also zero, there is no phase change. For this particular figure, we have non-dimensionalized all compositions with respect to the far-field liquid composition, and all temperatures with respect to the corresponding change in the liquidus temperature, $\Gamma$. It may be seen that as the far-field composition of the liquid is increased, the liquidus relation forces the interface temperature to decrease (as in case (*c*) of figure 5), and so melt begins to form from the solid. The corresponding increase in the composition of the melt at the interface accommodates the greater flux of solute supplied to the interface from the liquid. The reduction in the interface temperature increases the heat transferred to the interface from both the solid and liquid and therefore rate of phase change increases. This example isolates the role of composition dissolving, since in this example, when the liquid and solid have the same composition, there is no phase change.

The difference between melting and dissolving is very important in determining the form of the fluid convection which may arise at the interface. In the case of dissolving, the melt in the boundary layer above the interface has a rapid variation in composition and may be subject to a compositional Rayleigh–Bénard type of instability. In the case of melting, the melt in the boundary layer above the interface has nearly constant composition, but the temperature varies. If the density field is dominated by variations in composition, then this melt may be subject to a hybrid compositional Rayleigh–Taylor type of instability. We describe this in greater detail in the next section.

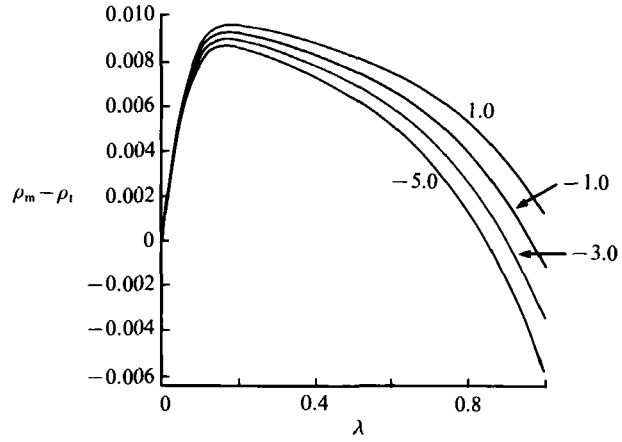


FIGURE 7. Density difference between the far-field melt and the interfacial melt as a function of the melting rate, $\lambda$, for $\hat{T}_s = 1.0, -1.0, -3.0, -5.0$, as shown on the curves, with $\alpha = 0.0001$ and $\beta = 0.01$.

## 3. Interfacial density and the convective regimes

In order to determine the stability of these diffusive solutions to convection in the melt, the density difference between the far-field melt and the interface was calculated. These calculations assume that the melt density satisfies the relationship.

$$\rho = \rho_0 - \alpha T + \beta C. \tag{3.1}$$

In general, the density depends much more strongly upon the composition than the temperature, $\alpha/\beta \sim 0.01$, and this is shown in the lines of constant density on the phase diagram (figure 1). We assume $\alpha > 0$ as is usually the case. In figure 7 we have plotted the density difference between the far-field melt, $\rho_m$, and the melt at the interface, $\rho_I$, as a function of $\lambda$, the similarity melting rate, in the case $\beta > 0$ corresponding to melting the less dense pure end-member solid. Curves are given for $\hat{T}_s = 1.0, -1.0, -3.0, -5.0$. For small values of $\lambda$, the density of the interfacial melt is smaller than the far-field melt. This is because the interfacial composition is smaller than that of the far-field melt (figure 4), and for small $\lambda$, the far-field melt temperature is relatively small (figure 2), so that the compositional differences dominate the density difference (3.1). However, as the melt temperature and hence $\lambda$ increase, the melt density eventually falls below that of the interface. We remark that in many laboratory situations the melt superheat is relatively small and so the interfacial melt will be buoyant relative to the far-field melt. However, as in figure 7, for much higher superheats, the interfacial melt will be relatively heavy. In contrast, when $\beta < 0$, which corresponds to melting the heavy pure end-member solid, the density of the hot far-field liquid is always less than that of the melt at the interface. Using the analysis of Turner (1979) and these results, we can now infer the convective regimes which may arise in the melt as a function of the net destabilizing Rayleigh number. The convective regimes (figures 8 and 9) depend upon whether the melt lies above or below the solid, and upon whether $\beta > 0$ or $\beta < 0$.

Three cases arise when the solid lies above the liquid. In all three cases the molten solid is colder than the underlying liquid and hence is always thermally unstable (ignoring effects such as the density maximum in water at 4 °C). If $\beta > 0$, the melt is compositionally stable and hence may be absolutely stable and float above the liquid (figure 8*a*). A double-diffusive interface then develops between the melt and

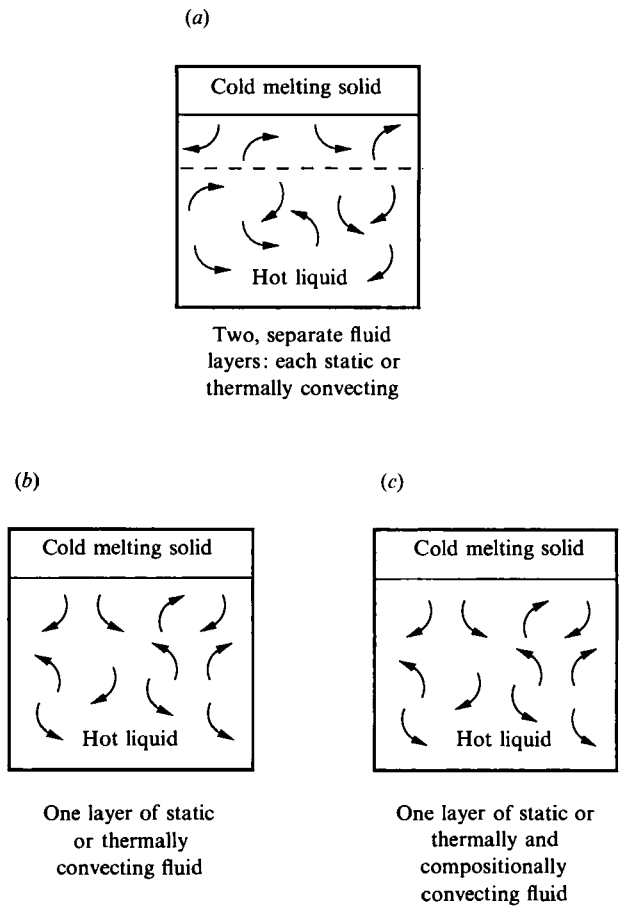


FIGURE 8. The modes of convection which may develop when solid is melted by an underlying liquid to produce melt which is (*a*) compositionally light and statically stable, but with each layer unstable to thermal convection for sufficiently high thermal Rayleigh number; (*b*) compositionally light but absolutely unstable due to thermal instability and so for sufficiently high net Rayleigh number convection sets in, and for very large net Rayleigh number this results in a well-mixed, convecting melt (Huppert & Sparks 1988*b*); and (*c*) compositionally heavy and absolutely unstable and so for sufficiently high total Rayleigh number convection sets in (cf. Turner 1979).

the liquid; either layer may begin to convect thermally if the thermal Rayleigh number for the layer becomes sufficiently large; the layers retain their identity, with heat transfer but little mass transfer across the interface (Turner 1979; Huppert & Sparks 1988*a*). This situation has been described in detail by Huppert & Sparks (1988*a*). However, again with $\beta > 0$, the thermal destabilization may exceed the stabilizing effect of composition; now the melt is absolutely unstable and for sufficiently large net destabilizing Rayleigh number, whole scale mixing may ensue (figure 8*b*); alternatively, in this case as the cold melt sinks it may heat up and become buoyant, rising back up to the interface (Huppert & Sparks 1988*a*). When $\beta < 0$, the composition of the molten solid is greater than the liquid, and so the interfacial melt is statically unstable due to both composition and temperature; for sufficiently large net Rayleigh number (Turner 1979), the melt will sink into the liquid and mix vigorously (figure 8*c*).

Three cases also arise when the solid is below the liquid. Now, the cold molten solid

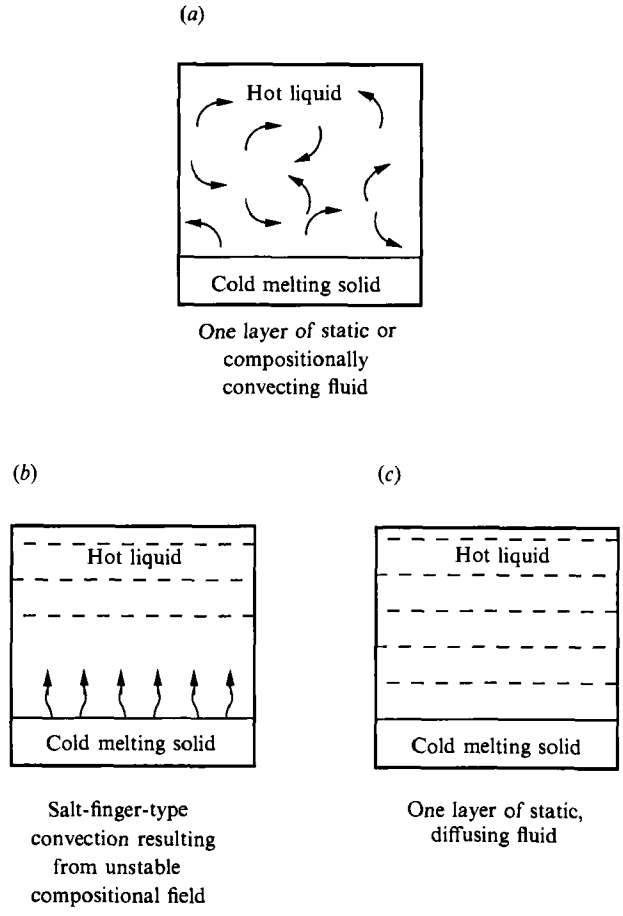


FIGURE 9. The modes of convection which may develop when a solid is melted by an overlying liquid producing melt which is (*a*) compositionally light and therefore absolutely unstable, leading to vigorous mixing for sufficiently large net Rayleigh number, (*b*) compositionally buoyant but statically stable, leading to salt-finger-type convection and (*c*) compositionally heavy and absolutely stable, leading to the diffusive melting of §2.

is thermally stable with respect to the overlying melt (again ignoring density reversals with temperature as occurs at 4 °C in water). If the molten solid is compositionally buoyant ($\beta > 0$), it may either be absolutely buoyant or statically stable. If the molten solid is absolutely buoyant, then, for sufficiently large net Rayleigh number, it will rise and mix into the overlying liquid as shown in figure 9(*a*). If $\beta > 0$, but the molten solid is statically stable relative to the overlying liquid, then it will be unstable to salt-finger type of convection, owing to the difference in the rate of diffusion of heat and salt (Turner 1979) and a convecting finger interface may develop (figure 9*b*). This situation has been discussed by Campbell (1986), Fang & Hellawell (1988), Huppert & Sparks (1988*c*) and Woods (1991). Woods noted that the finger convection may be suppressed, since the rate of melting and hence the supply of fresh but cold melt is small, giving rise to an essentially diffusive process. The third case arises when $\beta < 0$ and the molten solid is compositionally and therefore absolutely stable; in this case the system remains static for all time, figure 9(*c*), and all heat and mass transfer is diffusive; this is the situation which we analysed in §2.

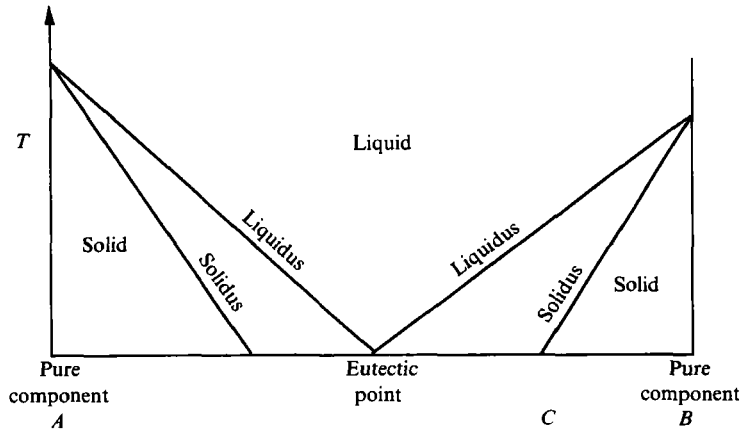


FIGURE 10. Phase diagram in the case in which both the liquidus and solidus depend upon temperature and composition.

## 4. Melting and dissolving a binary solid solution

We now consider the different situation in which the melting temperature of the solid, defined by the solidus curve, is a function of both the composition and temperature (figure 10). We restrict attention to solid of uniform composition; although the fundamental principles remain the same, the problem becomes considerably more involved if the solid composition is allowed to vary with depth. For simplicity, in the following discussion we describe solid of composition smaller than the eutectic composition; however, analogous results apply for solid of composition greater than eutectic.

In thermodynamic equilibrium, solid of composition $X$ may only rise above its solidus temperature $T_s(C)$ by selective melting, such that its composition changes and therefore the relevant local solidus temperature increases; such changes in the composition of the solid are controlled by diffusion of solute within the solid and therefore occur very slowly. However, owing to the much larger value of the thermal diffusivity in comparison to the solutal diffusivity in the solid, some constitutional superheating may develop in the solid just ahead of the interface. This process is similar to the development of constitutional supercooling in the liquid ahead of a solidifying interface, which is caused by the diffusion of solute in the liquid region and which results in the well-known morphological instability (Mullins & Sekerka 1964). Woodruff (1968) has carried out a full stability analysis for such a melting interface, including the diffusion of solute in both the solid and liquid phases. His results show that, in contrast to solidifying interfaces, melting interfaces generally remain stable and planar, owing to the very small diffusivity of solute in the solid and the stabilizing effect of solute diffusion in the liquid, even if there is some superheating in the solid ahead of the interface. Therefore, in the following analysis, we assume that the interface between the solid and liquid remains planar.

The composition of the solid and the melt at the interface are related by the partition coefficient $k$, such that

$$C_s\Big|_+ = kC_l\Big|_- . \tag{4.1}$$

In general $k$ is a function of the composition; however, for simplicity, in the following analysis we assume that it is a constant. The equations for the conservation of heat are identical to those describing the melting of a pure solid, presented in §2.

However, solute may now diffuse in the solid so that (2.1*d*) is replaced by a diffusion equation

$$\frac{\partial C}{\partial t} = D_s \frac{\partial^2 C}{\partial z^2} \quad \text{for} \quad z > h(t) \tag{4.2}$$

and the boundary condition (2.2*b*) is replaced by the more general relation

$$D_l \frac{\partial C}{\partial z}\bigg|_- - D_s \frac{\partial C}{\partial z}\bigg|_+ = -\dot{h} C_I (k-1), \tag{4.3}$$

where $C_I$ is the melt composition at the interface. This more general problem has solutions similar to (2.3*a–c*) but the composition in the solid now has the form

$$C = C_s + \left(\frac{k - C_s}{\operatorname{erfc}(\lambda/\delta)}\right) \operatorname{erfc}\left(\frac{\eta}{\delta}\right), \tag{4.4}$$

where $\delta = (D_s/\kappa_l)^{\frac{1}{2}} \ll \epsilon$. The eigenvalue relation (2.4*a*) is readily generalized to the form

$$\frac{\epsilon}{f(-\lambda/\epsilon)}(C_I - 1) + \frac{\delta}{f(\lambda/\delta)}(kC_I - C_s) = -\lambda(1-k)C_I. \tag{4.5}$$

This expression allows us to investigate the different phase change regimes from solid into liquid, in order to generalize the discussion of §2.

### 4.1. *The melting regime*

Whenever the far-field melt has a large superheat such that $\lambda \sim O(1)$ and the rate of melting is determined by the thermal diffusivity, then the composition of the melt at the interface $C_I \sim C_s$, the solid composition. Therefore, in this case of rapid phase change, a layer of molten solid, with the same composition as the far-field solid forms behind the melting front, and there is a compositional boundary layer embedded in the liquid, at the original position of the solid. This is identical to the melting regime described in §2 and shown in figure 3(*b*). This solution regime is sketched in figure 11(*a*).

The narrow compositional boundary layer ahead of the melting interface, in the solid, as given by (4.4) is purely an artifact of the assumption that the solid remains in equilibrium at the interface with the liquid. Apart from this narrow compositional boundary layer in the solid, we can obtain an identical solution if we assume that the solid is of fixed composition and allow the solid to support superheat. Whether such a compositional boundary layer develops in reality must be tested experimentally, since solid can support some superheat before melting. In either case, the solid just ahead of this compositional boundary layer becomes superheated owing to the more rapid diffusion of heat than solute in the solid.

### 4.2. *The dissolving regime*

As the melt superheat is reduced, the rate of phase change decreases and eventually $\lambda \sim O(\epsilon)$. In this regime, (4.5) reduces to the form

$$\frac{\epsilon}{f(-\lambda/\epsilon)}(C_I - 1) = \lambda(C_s - C_I) \tag{4.6}$$

which is identical to (2.4*b*). As $\lambda$ decreases, the dimensionless composition of the melt at the interface, $C_I$, evolves from that of the far-field solid towards that of the far-

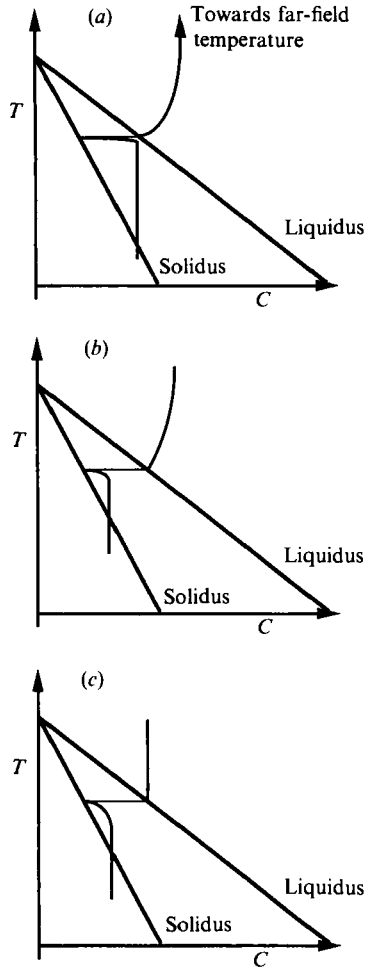


FIGURE 11. Three situations which may arise when a binary solid is placed in contact with a binary liquid and melt is produced from the solid. In these figures, the solid is of smaller composition than the liquid and is (*a*) melting; (*b*) dissolving; (*c*) slowly dissolving. The solid portions of the path represent the physical path through the system, while the thinner portion represents the change in composition as we move from solid to melt.

field liquid, which has dimensionless value unity. This is very similar to the dissolving regime described in §2, and the composition of the melt at the interface changes according to the graph shown in figure 4. The composition of the melt at the interface evolves towards that of the liquid as the dissolution rate decreases because the rate of production of melt is now comparable to the rate of diffusion of solute in the liquid (as in figure 3*a*). This solution regime is sketched in figure 11 (*b*).

Again, the imposition of thermodynamic equilibrium upon the solid at the interface with the liquid results in the prediction of a very narrow boundary layer in the solid just ahead of the interface; however, now the solid composition adjusts diffusively from the far-field solid composition $C_s$ to the value $kC_l$ across this boundary layer. However, as in the melting regime, (4.6), which is valid in the limit $\lambda \gg \delta$, shows that apart from the narrow compositional boundary layer in the solid, we would obtain the same solution by assuming that (i) the solid was of fixed composition and (ii) before melting the solid can support superheat.

As the superheat of the melt is further reduced, $\lambda$ decreases such that $\lambda \ll \epsilon$. In this case, (4.5) reduces to the simple form $C_I = 1$, so the composition of the melt at the interface becomes equal to that of the liquid in the far field. This regime represents *slow dissolution* of the solid and is sketched in figure 11(*c*). In order that the solid at the interface remains in equilibrium, the compositional boundary layer in the solid effects the solute transfer to or from the solid at the interface as the solid changes phase into melt. The three types of solution shown in figure 5 may develop in this slow dissolution regime.

Note that in the slow dissolution regime, the composition of the solid at the interface may be greater or smaller than that of the solid in the far field, depending upon the composition of the far-field melt relative to that of the far-field solid, since the solutal diffusivity in the solid is much smaller than that in the liquid. As in §2, we deduce from the thermodynamic relation (2.4*b*) that, in the dissolving regime, $T_m - 2(1-C_m) + T_s = o(\epsilon)$.

Verhoeven & Gibson (1971*a*,*b*) carried out some experiments in which Sn–Si and Sn–Bi alloys were directionally melted in a crucible. At a particular point in each of their experiments, the material was rapidly quenched to preserve the structure of the phase change interface and the resulting quenched solid was examined by metallographic techniques. Based upon evidence that small pockets of partial melt developed ahead of the main solid/liquid interface, Verhoeven & Gibson (1971*a*,*b*) deduced that the solid became constitutionally superheated ahead of the melting interface. In the Sn–Bi experiments this partial melt region took on several forms: at high temperature gradients, a network of interconnected cylindrical channels developed, while at lower temperature gradients a cellular interface type structure developed. We believe that these pockets of partial melt formed at grain boundaries, which act as nucleation sites for melting. The melting which occurs at these grain boundaries will be controlled by kinetic effects and so we expect that this solid can support some superheat.

However, the photographs from the experiments of Verhoeven & Gibson indicate that there are only a relatively small number of pockets of partial melt, corresponding to the finite number of grain boundaries. Furthermore, the spacing between grain boundaries is relatively large compared to the very small lengthscale of diffusion of solute in the solid over the timescale of the propagation of the phase change front. Therefore, the majority of the solid behind the liquid interface remained as superheated solid of the original solid composition and the majority of the phase change occurred at the planar interface between the solid and liquid. These observations are in general accord with the model we described above. In our model, we ignore the development of pockets of partial melt ahead of the main interface between the solid and liquid. To leading order, this is a valid approximation because they represent only a very small fraction of the solid, and therefore, they have only a negligible effect upon the conservation of heat. The observation of such pockets of melt is important, however, since it confirms our model of the development of superheat in the solid ahead of the compositional boundary layer.

### 4.3. *Implications for convection*

Owing to the similarity in the phase change processes, much of the discussion of §3 concerning the possible modes of convection which may arise during the melting of a pure solid also applies during the melting of a binary solid solution. However, we are able to extend the discussion to consider both melt and solid of arbitrary binary composition.

## 5. Conclusions

We have investigated the melting of a binary alloy into a binary melt in two situations. First we considered the case when solid composed of one pure end-member is placed in contact with a binary liquid. We have obtained similarity solutions which describe the diffusion-controlled phase change of the solid into melt. If the melt superheat is very large, the process is controlled by the thermal diffusivity; the composition of the melt at the interface equals that of the solid and so the interface temperature equals the maximum melting temperature of the solid. We call this process *melting*. As the melt superheat is reduced, the temperature of the interface eventually decreases below this maximum melting temperature; therefore, the composition of the melt at the interface differs from that of the solid since it is constrained by the liquidus relationships. Now, the phase change becomes controlled by the compositional diffusivity in the liquid, because solute must be supplied to the melt at the same rate as it changes phase. We describe this process as *dissolving*. During dissolving, the composition of the liquid at the interface differs from both that of the solid and liquid and so we conclude that the process of dissolving is driven by chemical disequilibrium. Only when the composition of the liquid at the interface equals that of the far-field liquid can the phase change cease. As a consequence, when the temperature of the far-field solid exceeds the liquidus temperature corresponding to the far-field liquid composition, the solid always dissolves into the liquid if the system is to remain in thermodynamic equilibrium.

We have discussed the convective stability of melting and dissolving in the cases in which the solid is melted from either above or below and the melt is relatively light or heavy compared to the molten solid. During the melting process the melt may exhibit salt-finger-type convection, double-diffusive type convection, fully turbulent convection or it may remain static, as summarized in figures 8 and 9.

Next we analysed the situation in which the solid is a solution of both components, with the melting temperature of the solid (the solidus) a function of both the temperature and composition of the solid. We have shown that the simple results for a pure solid may be simply adapted to model this situation as well. Owing to the very small solutal diffusivity in the solid, the composition of the melt at the interface is determined by the rate of diffusion of solute in the liquid in comparison with the rate of phase change. When the rate of phase change is very large, the composition of the melt at the interface equals that of the solid in the far field; this is the melting regime. When the rate of phase change decreases and is controlled by the rate of diffusion of solute in the liquid, the composition of the melt at the interface evolves towards the composition of the melt in the far field. This corresponds to the dissolving regime.

As one example, these results have important implications for the intrusion of a magma of one temperature and composition into a magma chamber whose bounding walls are composed of magma of different composition and temperature. The model provides simple constraints which determine whether the solid walls of the chamber will melt back. Furthermore, we have shown that when a solid changes phase rapidly, the melt so produced has the same composition as the solid, while if the phase change occurs more slowly then the melt produced from the solid may have a different composition from that of the solid, depending upon the composition of the liquid.

This work has benefitted from discussions with Professors H. E. Huppert and M. G. Worster and very careful, helpful and critical reviews from three anonymous

referees. I would like to thank the Green Foundation for support as a Green Scholar at the Institute of Geophysics and Planetary Physics, Scripps Institute of Oceanography, where I commenced this study.

## REFERENCES

BRUCE, P. M. & HUPPERT, H. E. 1989 Thermal controls of basaltic fissure eruptions. *Nature* **342**, 665–667.

CAMPBELL, I. 1986 A fluid dynamic model for the formation of pot-holes in the Merensky reef. *Econ. Geol.* **81**, 1118–1125.

CARSLAW, H. S. & JAEGAR, J. C. 1986 *Conduction of Heat in Solids*. Oxford University Press.

FANG, D. & HELLAWELL, A. 1988 The surface morphology of crystals growing under solutions of different densities. *J. Cryst. Growth* **92**, 364–370.

HILL, J. M. 1987 *One-dimensional Stefan Problems: An Introduction*. Longman.

HUPPERT, H. E. 1989 Phase changes following the initialisation of a hot turbulent flow over a cold solid surface. *J. Fluid Mech.* **198**, 293–320.

HUPPERT, H. E. & SPARKS, R. S. J. 1988*a* Melting the roof of a turbulently convecting chamber. *J. Fluid Mech.* **188**, 107–131.

HUPPERT, H. E. & SPARKS, R. S. J. 1988*b* The generation of granitic magmas by intrusion of basalt into continental crust. *J. Petrol.* **29**, 599–624.

HUPPERT, H. E. & SPARKS, R. S. J. 1988*c* The fluid dynamics of crustal melting by injection of basaltic sills. *Proc. R. Soc. Edin., Earth Sci.* **79**, 237–243.

HUPPERT, H. E. & WORSTER, M. G. 1985 Dynamic solidification of a binary alloy. *Nature* **314**, 703–707.

KERR, R. C., WOODS, A. W., WORSTER, M. G. & HUPPERT, H. E. 1989 Disequilibrium and macrosegregation during the solidification of a binary melt. *Nature* **340**, 357–362.

KERR, R. C., WOODS, A. W., WORSTER, M. G. & HUPPERT, H. E. 1990 Solidification of an alloy cooled from above. Part 2. Non-equilibrium interfacial kinetics. *J. Fluid Mech.* **217**, 331–348.

KURZ, W. & FISHER, D. J. 1986 *Fundamentals of Solidification*. Trans. Tech. Publications.

LEWIS, E. L. & PERKINS, R. G. 1986 Ice pumps and their rates. *J. Geophys. Res.* **C91**, 11756–11762.

MULLINS, W. W. & SEKERKA, R. F. 1964 Stability of a planar interface during the solidification of a binary alloy. *J. Appl. Phys.* **35**, 444–451.

TURNER, J. S. 1979 *Buoyancy Effects in Fluids*. Cambridge University Press.

VERHOEVEN, J. D. & GIBSON, E. D. 1971*a* Interface stability of the melting solid–liquid interface. I. Sn-Sb alloys. *J. Cryst. Growth* **17**, 29–38.

VERHOEVEN, J. D. & GIBSON, E. D. 1971*b* Interface stability of the melting solid–liquid interface. II. Sn-Bi alloys. *J. Cryst. Growth* **17**, 39–49.

WOODRUFF, D. P. 1968 The stability of a planar interface during the melting of a binary alloy. *Phil. Mag.* **17**, 283–294.

WOODS, A. W. 1991 Fluid mixing during melting. *Phys. Fluids* A **3**, 1393–1404.

WOODS, A. W. & HUPPERT, H. E. 1989 The growth of compositionally stratified solid above a horizontal boundary. *J. Fluid Mech.* **199**, 29–54.

WORSTER, M. G. 1986 Solidification of an alloy from a cooled boundary. *J. Fluid Mech.* **167**, 481–501.

WORSTER, M. G. 1991 Natural convection in a mushy layer. *J. Fluid Mech.* **224**, 335–340.